



This is a repository copy of *Entropy of Molecular Binding at Solvated Mineral Surfaces*.

White Rose Research Online URL for this paper:
<http://eprints.whiterose.ac.uk/84099/>

Version: Accepted Version

Article:

Freeman, C.L. and Harding, J.H. (2013) Entropy of Molecular Binding at Solvated Mineral Surfaces. *Journal of Physical Chemistry C*, 118 (3). 1506 - 1514. ISSN 1932-7447

<https://doi.org/10.1021/jp407122u>

Reuse

Unless indicated otherwise, fulltext items are protected by copyright with all rights reserved. The copyright exception in section 29 of the Copyright, Designs and Patents Act 1988 allows the making of a single copy solely for the purpose of non-commercial research or private study within the limits of fair dealing. The publisher or other rights-holder may allow further reproduction and re-use of this version - refer to the White Rose Research Online record for this item. Where records identify the publisher as the copyright holder, users can verify any specific terms of use on the publisher's website.

Takedown

If you consider content in White Rose Research Online to be in breach of UK law, please notify us by emailing eprints@whiterose.ac.uk including the URL of the record and the reason for the withdrawal request.



eprints@whiterose.ac.uk
<https://eprints.whiterose.ac.uk/>

Entropy of Molecular Binding at Solvated Mineral Surfaces

Colin L. Freeman^{1*} and John H. Harding¹

¹ Department of Materials Science and Engineering, University of Sheffield, Sheffield, UK

November 18, 2013

Abstract

We present thermodynamic integration simulations for the binding of mannose and methanoic acid onto the {10.4} calcite surface producing free energy of binding values of -2.89 and -1.64 kJmol⁻¹ respectively. We extract the entropy of binding from vacuum based simulations and use these values to determine the entropy of binding for surface water molecules which is ~ 6 Jmol⁻¹K⁻¹.

Keywords: Free energy; Computer Simulation; Biomineralisation; Adsorption.

*Address correspondence to this author. Phone: +44 (0)114 222 5965. Fax: +44 (0)114 222 5943. E-mail: c.l.freeman@sheffield.ac.uk

1. Introduction

Understanding the interactions between molecules and surfaces is vital for a wide range of fields such as crystal growth, catalysis and purification. Theoretical methods are increasingly being applied to tackle this challenge with great success. Modelling the interface between a surface and adsorbate is complex. At the heart of these calculations is the desire to calculate adsorption free energies. These values indicate the likelihood of molecular attachment, surface selectivity and whether preferential binding occurs at localised defects. Although configurational energies are produced from standard simulations, the entropy cannot be determined as it is not a statistical average of the system. Depending on the system, entropy can be a vital component of any binding, particularly when large molecules (with a variety of conformations and configurations) or solvent molecules at the surface are involved. In these situations the entropy change of the system may be very large and the entropy may become the dominant factor in the *free* energy of adsorption.^{1,2}

There are many different methods available to calculate the free energy of a system and thereby include the entropic term in the free energy of binding. These include thermodynamic integration (TI),³ umbrella sampling,^{4,5} radial distribution methods⁶ and metadynamics.⁷ Each of these methods has different merits, for example metadynamics, although biasing the system to explore particular order parameters does not force the system to adopt a particular trajectory which can make it difficult to ensure that the desired phase space is explored. Although these methods can provide a free energy it is rarely simple to separate this energy into the enthalpic and entropic components.

Recent work on molecular binding to calcite surfaces e.g.^{8,9} has suggested that the water on the calcite surface partially controls the binding. The strong water-calcite interactions create tightly bound water layers, the disruption of which, via molecular binding, generates an enthalpic penalty. This has led to the lowest energy molecular binding configurations frequently demonstrating relatively little contact with the calcite surface as this minimises the enthalpic penalty associated with disrupting the water. This result has been most striking in our simulations of the protein, Ovocleidin-17 (OC-17), binding to calcite surfaces,^{10,11} where the lowest energy configuration was found to have three amino acid residues in contact with the surface while the highest energy binding configuration had nine residues. Obviously in these two configurations the number of water molecules displaced from the surface varied; the protein in the highest enthalpy configuration displaced ten more water molecules from the surface than in the lowest enthalpy configuration. Therefore the entropy change from the binding should be more favourable for the highest enthalpy configuration since the water is moving from an ordered surface layer

to the disordered bulk. Given this, it is possible that the free energy of binding may not be simply an extrapolation of the enthalpy since the enthalpy favours one configuration and entropy the other. The prediction of the free energy of binding for these processes would be highly desirable. Direct free energy calculations are, however, too expensive for these large systems. An alternative is to apply an entropy correction to the enthalpic component to generate an estimate for the free energy or a *pseudo*-free energy.

At its most basic an NVT molecular dynamics (MD) calculation using the TI method will return the Helmholtz free energy, A ,

$$A = U - TS, \tag{1}$$

where U is the internal energy of the system and S is the entropy. The entropy relating to a molecule binding to a surface will be a combination of four different components

1. The entropy loss as the molecule is bound to the surface and loses much of its configurational freedom.
2. The entropy gain as solvent molecules previously bound to the surface are displaced into the solution.
3. An entropy change in the surface atoms as they become more or less mobile with the new binding configuration.
4. An entropy gain as solvent molecules bound to the molecule in solution are released.

A physisorbed molecule is unlikely to induce any significant change in the vibrations of the surface atoms (unless the attaching molecule causes dissolution) so (3) can be largely ignored. Unless strongly bound solvent molecules (e.g. structured water) are displaced on binding, then (4) will be relatively small. Therefore it is reasonable to assume that the main factors dominating the entropy change will be (1) and (2).

Models have been proposed for estimating the entropy of large molecules such as the Schlitter approach¹² where the modes of the molecule are calculated and used to determine the entropy of the molecule. This method has been successfully applied to different configurations of DNA molecules to determine lowest energy configurations.¹³ The large number of modes available within molecules with less rigid structures than DNA, for example proteins, limits the application of this method to these particular molecules but it remains a very successful technique for accessing entropic contributions. A similar method cannot be used for solvent molecules as much of the entropy change is not due to variations in harmonic modes. Here a large degree of entropy gain comes from librational entropy and the amount will vary between solvent and surface. Irudayam *et al*^{14,15} determined the entropy of water

molecules via a partition function with each degree of freedom described with a potential fitted from confinement simulations. This method has proved extremely useful in analysing solvation of molecules and water components in different systems. Another alternative is a two-phase method where the density of states is broken down into gas phase (to cover the fluid effects) and solid phase (for quantum effects) components. The density of states of the liquid phase is assumed to be a superposition of the gas and solid. This has been successfully implemented by Lin *et al*^{16,17} to calculate the entropy of water in complicated systems such as a bilayer.¹⁸ Other methods in the literature include the construction of the non-ideal component of the entropy via configurational sampling¹⁹ where an approximation is made that of “hypothetical scanning”. As yet, to the authors knowledge, none of these methods has been applied to solvent molecules at solid-liquid interfaces which is the challenge of our present study.

The method proposed by Smith *et al*^{20,21} and other similar ones in the literature^{22,23} describes the entropy between two states (of a TI) as a correlation function between the ensemble averages of the potential (or configuration) energy, U , and its derivative with respect to the TI parameter, λ .

$$-T\Delta S_{0\rightarrow 1} = \frac{1}{kT} \int_{\lambda=0}^{\lambda=1} d\lambda [\langle U \frac{\delta U}{\delta \lambda} \rangle_{\lambda} - \langle U \rangle_{\lambda} \langle \frac{\delta U}{\delta \lambda} \rangle_{\lambda}]. \quad (2)$$

This method provides a powerful tool for extracting the entropic component of the free energy. We can assume that the bulk of this entropy is derived from the molecular change (1) and surface water (2). We propose to obtain the separation of these entropic terms by performing the same TI for the molecular adhesion with an identical trajectory in vacuum (no solvent present) where the variable λ is the separation of the molecular centre of mass and the calcite surface. Using equation 2 on this TI will yield the entropy change for the molecule only. Assuming that the molecule does not adopt a significantly different configuration during the simulations with and without the solvent present (which can be ensured by forcing the molecule along the same trajectory and imposing restrictions on its flexibility) then the differences between the entropy component of the solvated and vacuum simulations should approximate to the entropy of the solvent. With a known value for the solvent entropy it should be possible to apply this value to other simulations to estimate the free energy of binding.

We present TI simulations for two small molecules - mannose and methanoic acid adsorbing to the (10.4) calcite surface in vacuum and water. These two molecules are chosen for two main reasons: firstly, they contain particularly interesting functional groups - alcohol/acid - which have been shown to have strong interactions with both water layers and calcite surfaces and; secondly their sizes - the relatively larger size and rigid framework of the mannose molecule makes it ideal for looking at the displacement

of multiple water molecules from the surface compared to the acid molecule. Using a flexible large molecule would present many configurational issues and be difficult to regulate within a TI simulation. Using these simulations we extract the entropy of displacing a water molecule from the calcite surface and use this to estimate entropy effects in larger simulations.

2. Methods

Our simulations used classical methods with the potential sets taken from the all atom AMBER forcefield set²⁴ for the mannose and methanoic acid molecules. The Pavese forcefield^{25,26} was used to model the calcite mineral and the water was treated with the TIP3P model.²⁷ Interactions between the solvent or molecule and the mineral were taken from Freeman *et al.*²⁸

Slabs of (10.4) calcite were constructed from pre-optimised surface structures using the METADISE (Minimum Energy Techniques Applied to Dislocation Interface and Surface Energy)²⁹ code. The slabs consisted of 960 formula units which gave a surface area of 2450 Å² and a thickness of 8 layers. A single mannose or methanoic acid molecule was solvated in 2495 water molecules and allowed to relax before the molecule and water box were placed in contact with the surface. The simulation box was constructed so as to ensure that both surfaces were solvated and no vacuum was present. The box size was chosen to ensure the bulk density of water at 300 K (0.99 g/cm³) was reproduced.

Molecular dynamics (MD) simulations were all performed using the DL_POLY code version 2.18³⁰ with an NVT ensemble using a relaxation time of 0.1 fs and 1 fs timesteps. A temperature of 300 K was used for the simulations. Three separate MD simulations with different start points were performed on each molecule to allow the molecules to adsorb onto the surface. From these simulations the lowest energy configuration for each molecule was then taken as the final adsorbed position for the molecules as part of the TI.

For the TI the mannose molecule was displaced in a series of steps of 0.3 Å in a direction perpendicular to the surface. Displacements of 0.15 Å were used for the methanoic acid molecule as its smaller size meant relaxations varied more significantly with its position. At each step (including the adsorbed position) a full MD simulation was run until the system demonstrated a converged energy. This was defined as a 0.2 ns bins producing energies within ± 20 kJmol⁻¹ of the final 1ns average. The errors are not shown on the graphs for clarity. In order to ensure that the molecule remained fixed at this point all the carbon atoms within the molecule (i.e. one in the methanoic acid and six in the mannose) were kept fixed. Freezing these atoms was necessary to ensure that the same trajectory was followed by the molecules

toward the surface in both the solvated and vacuum simulations if this was not the case then a different adsorption process would potentially take place as the preferred minimum energy configurations may be different between vacuum and solvated where displaced water contributes significantly to the final energy. Different trajectories and different final adsorption sites would invalidate the comparison between the solvated and vacuum simulations as the molecular entropy would be very different in the two cases making extraction of the entropy component of the water impossible. This method does mean that it is unlikely the molecules are following the lowest energy pathway towards/from the surface and relaxations will potentially be missed. Given that the primary goal of the process is to extract the entropic water contribution rather than model the TI of molecules on a calcite surface this is not a major problem. The process was continued until both molecules had been moved by 5.4 Å (16 steps) away from the surface. The same process was then performed for each molecule in an identical box with no water molecules present.

3. Results & Discussion

3.1 Mannose Adsorption The configurational energy at each point can be seen in Figure 1 for the mannose molecule in water and vacuum. An adsorption energy of -73.6 kJmol^{-1} for the solvated mannose demonstrates that adsorption is energetically favourable and agrees well with other simulations of polysaccharides on calcite surfaces.³¹ The adsorption energy for the vacuum simulation is approximately double, $-157.0 \text{ kJmol}^{-1}$, which shows the displacement of water from the calcite surface as the molecule binds imposes a significant energetic penalty as has been reported elsewhere e.g.^{8,9}

In the vacuum case there is no barrier to adsorption, as would be expected and the only increase in configuration energy occurs when the molecule is pushed into very close proximity with the surface. The configurational energy converges to a relatively constant value at $\sim 7.5 \text{ Å}$ from the surface which suggests that the long range interactions between the molecule and surface are converging to zero at this separation.

In the solvated system there is a clear barrier towards adsorption at approximately 5.1-6.6 Å from the surface (labelled 1 in Figure ??A. This broad barrier spans $\sim 1.5 \text{ Å}$ with a height of $\sim 50 \text{ kJmol}^{-1}$ from the configuration energy of the mannose in the bulk water. The barrier stems from the tightly bound surface water molecules that must be displaced by the mannose for it to fully adsorb onto the surface and has been observed for other surface adsorptions.³ Examining Figure 2B, this high energy region relates to when the alcohol groups of the mannose molecule, rather than the backbone atoms, enter the tightly bound double layer of water molecules. As the molecule is brought into this water layer the oxygen and hydrogen atoms of the alcohol groups will interact with the water molecules disrupting the

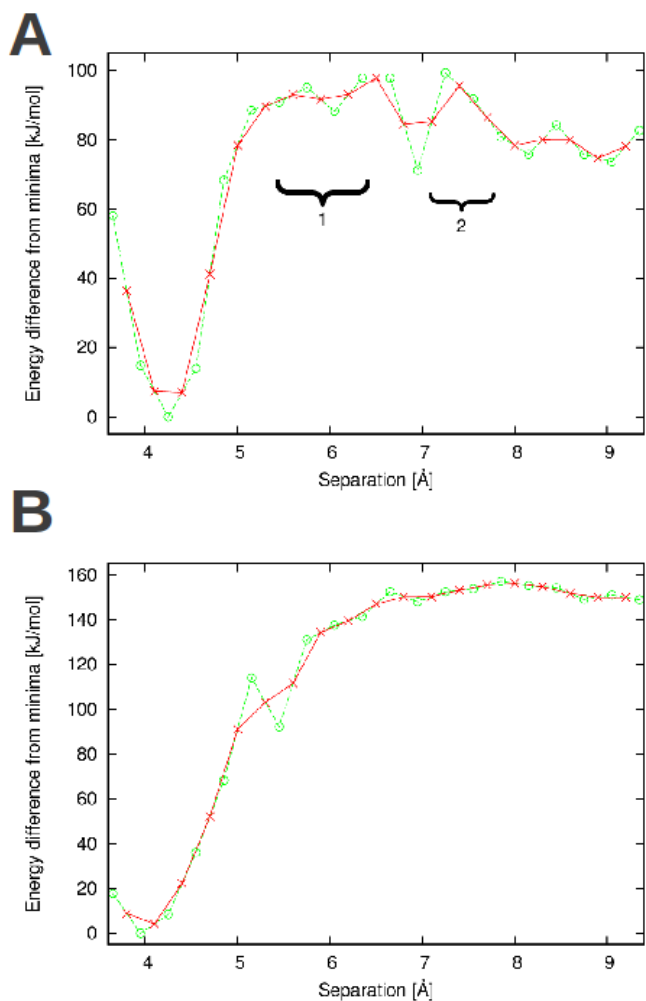


Figure 1.: Variation of configurational energy with separation of the mannose molecule from surface in (a) water and (b) vacuum. The separation from the centre of mass of the mannose to the surface is recorded. The final data points are shown as green circles and the integration points for the TI obtained by the numerical average of the neighbouring points are shown as red crosses.

interactions between the water molecules and surface atoms. This process is energetically unfavourable and is reflected in the adsorption plots. It is interesting that only one large broad barrier is found for the interactions with the surface double layer as in some previous simulations two distinct energy barrier peaks have been recorded.³ A small energy well of approximately 10 kJmol^{-1} can be seen approximately half-way across the barrier at 6.0 \AA but this is too small to define two separate barriers. The single barrier suggests that the mannose molecule must interact with both water layers simultaneously. The size of the mannose molecule does not appear to be responsible for this as most of the backbone of the molecule is not within the water layers. It may be due to the multiple functional groups on the mannose molecule which means that an alcohol group will always be in a position to interact with each of the

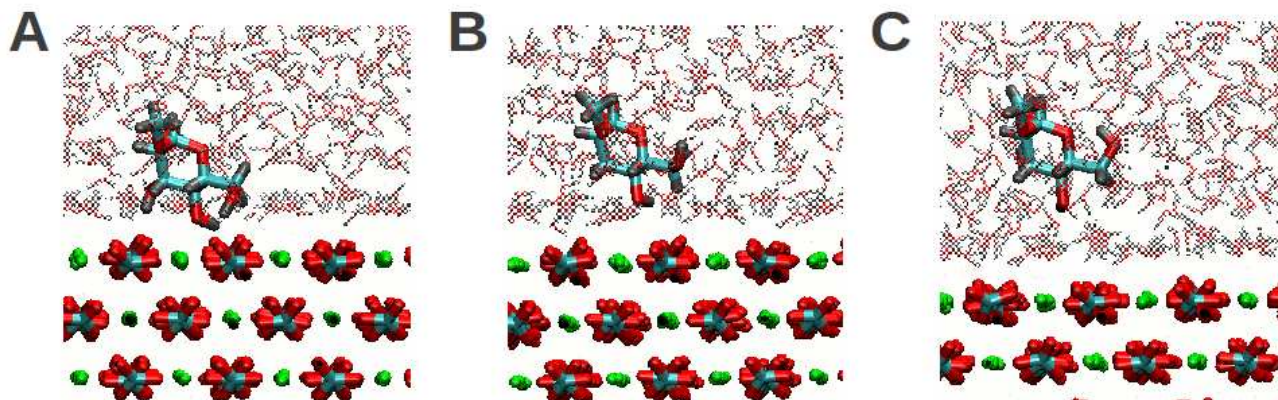


Figure 2.: Images of mannose binding at the calcite surface at (a) 4.25 (b) 5.45 and (c) 8.45 Å from the centre of mass of the mannose to the surface.

water layers, unlike for smaller molecules that have a single functional group.

There is a second barrier from 7.2-7.8 Å (labelled 2 in Figure ??A) from the surface which is only ~ 0.6 Å wide but still ~ 50 kJmol $^{-1}$ high. This appears to relate to the third water layer which is observed on the calcite surface. This layer is not as tightly bound as the first and second water layers which may explain why the barrier is narrower since the layer is not as organised and disruption of this water layer has a smaller overall energetic penalty. Beyond 8.2 Å from the surface the molecule appears to be interacting with bulk-like water and has reached a standard solvated environment.

3.2 Methanoic Acid Adsorption The variation of the configurational energy at each point can be seen in Figures 3A and 3B for the acid molecule in water and vacuum respectively. The adsorption energy is -58.8 kJmol $^{-1}$ for the solvated acid, demonstrating favourable binding. For the vacuum simulations the adsorption energy is -94.5 kJmol $^{-1}$, which is greater than the solvated value. This suggests that the displacement of water by the acid molecule is an important contribution to the binding energy though not as significant as for the mannose molecule.

The potential energy surface for the adsorption of the acid molecule is much more variable than that of the mannose. There are a large number of small peaks and troughs as the acid approaches the surface. Two main barriers can be identified in the plot. The first barrier (labelled 1 in Figure 3) begins at 5.5 Å with a height of ~ 30 kJmol $^{-1}$ and a width of 0.6 Å. The second energy barrier (labelled 2 in Figure 3) to adsorption of the acid molecule has a width of ~ 1.0 Å and a height of ~ 40 kJmol $^{-1}$. The positions of these barriers appear to be due to the first and second water layers of the surface water. It can be seen that the acid group of the molecule is interacting with the first water layer in Figure 4B although this interaction is not so clear within Figure 4C which corresponds to barrier 1. Unlike the case of the mannose

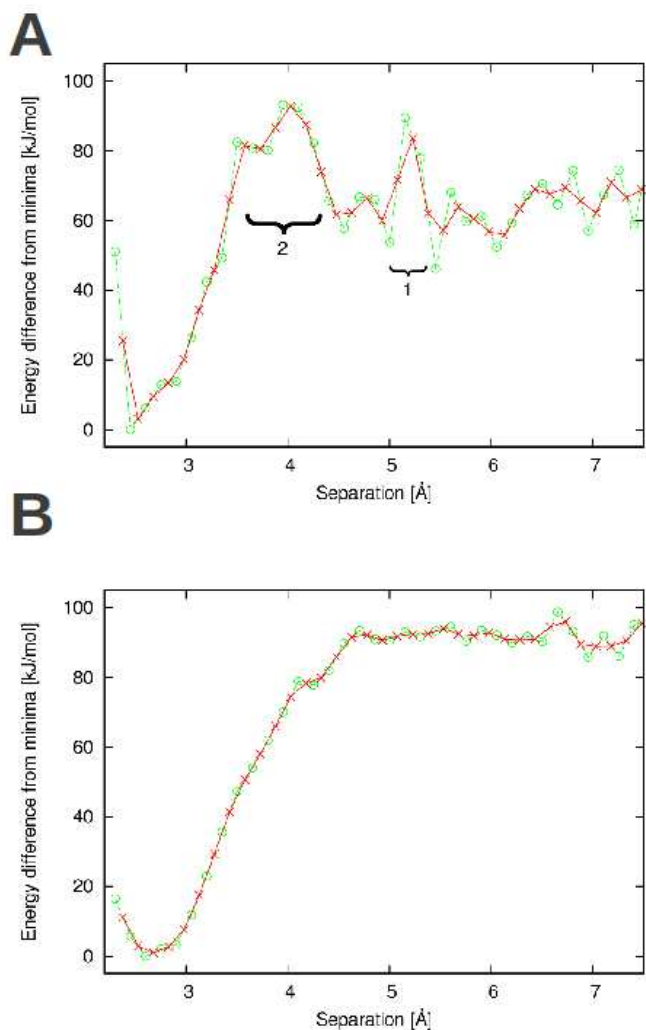


Figure 3.: The variation of configurational energy with separation of the methanoic acid molecule from surface in (a) water and (b) vacuum. The final data points are shown as green circles and the integration points for the TI obtained by the numerical average of the neighbouring points are shown as red crosses.

molecule where the interactions with the two water layers appeared merged, the acid molecule interacts with each layer individually and the larger second barrier corresponds to the tighter bound first water layer. There is some evidence of a third barrier which could link to the third water layer beginning at ~ 6.9 Å. This barrier is similar in height to the acid molecule in bulk water and only occurs due a fall in the configurational energy as the acid molecule begins to approach the surface. Based on the bulk energies this barrier is only ~ 10 kJmol^{-1} and cannot be considered definitive within the error range of the data.

The presence of only one functional group on the acid molecule may mean it is able to pass through the water layer without causing major disruption and therefore avoid some of the energetic penalties associated with the mannose molecule. This may explain why the binding of the acid has smaller, nar-

lower barriers than the mannose. The binding of a water molecule which is obviously also comparatively small showed only two barriers from the first and second water layers.³

Comparison between the mannose and methanoic acid molecule binding demonstrates a potentially interesting feature of molecular design affecting binding. The single functional group of the acid molecule may lead to smaller barriers as it causes a smaller disruption of the water layers at the calcite surface compared to the mannose molecule. The final adsorption energies, however, are larger for the mannose molecule which is able to generate more favourable interactions with the surface. For OC-17 it was noted that the main binding residues were the arginine residues which are structural long thin chains ending in amine groups.¹⁰ The structure of these residues would minimise the disruption of the water layers as they approach the surface ensuring a smaller energy barrier but would also achieve a negative adsorption energy by having multiple binding sites in contact with the surface.

3.3 Free Energy of Adsorption Using the TI method we calculate the free energy of binding to be -2.89 kJmol^{-1} and -1.58 kJmol^{-1} for the mannose and methanoic acid molecules respectively. Given that the simulations with fully mobile molecules did show a migration of the molecules to the surface and their attachment for the remainder of the simulation the binding would be expected to have a negative free energy.

3.4 Entropy of Adsorption The entropy change of binding can then be calculated via the method described in ref²⁰ as $15.62 \text{ JK}^{-1}\text{mol}^{-1}$ and $10.45 \text{ JK}^{-1}\text{mol}^{-1}$ for the mannose and methanoic acid respectively.

Plots of the entropy variation with separation from the surface for the mannose molecule is shown in Figure 5A. It is possible to examine the entropy changes that occur at each step in the TI as a guide to the entropic changes occurring during the binding process. For the mannose molecule an increase is observed as the mannose molecule enters the third water layer which relates to the disruption of this water layer. A large decrease can then be seen for the system when the mannose molecule is between the third and second layers. It would be expected that this comes from the reduced freedom of the mannose molecule imposed by the structured water layers that surround it. As the mannose enters the second water layer the entropy of the system again increases. There is finally a region with approximately zero entropy change before another increase in the entropy. We can speculate that this relates to the loss of entropy of the mannose molecule as it reaches its adsorbed position before displacing the final water molecules from the surface.

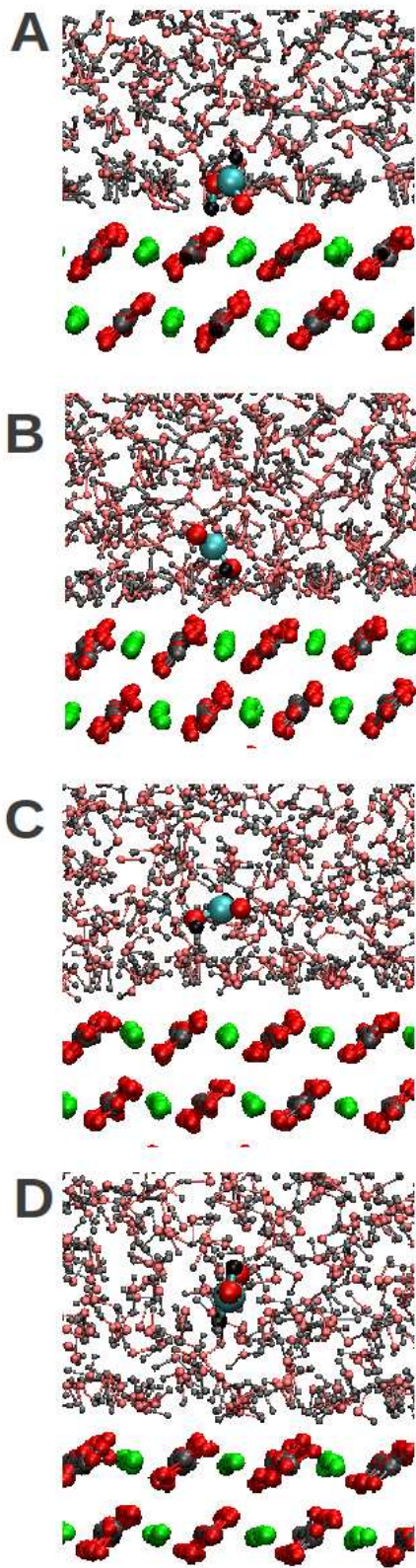


Figure 4.: Images of methanoic acid binding at the calcite surface at (a) 2.6 (b) 4.1 (c) 5.0 and (d) 6.2 Å from the centre of mass of the acid to the surface.

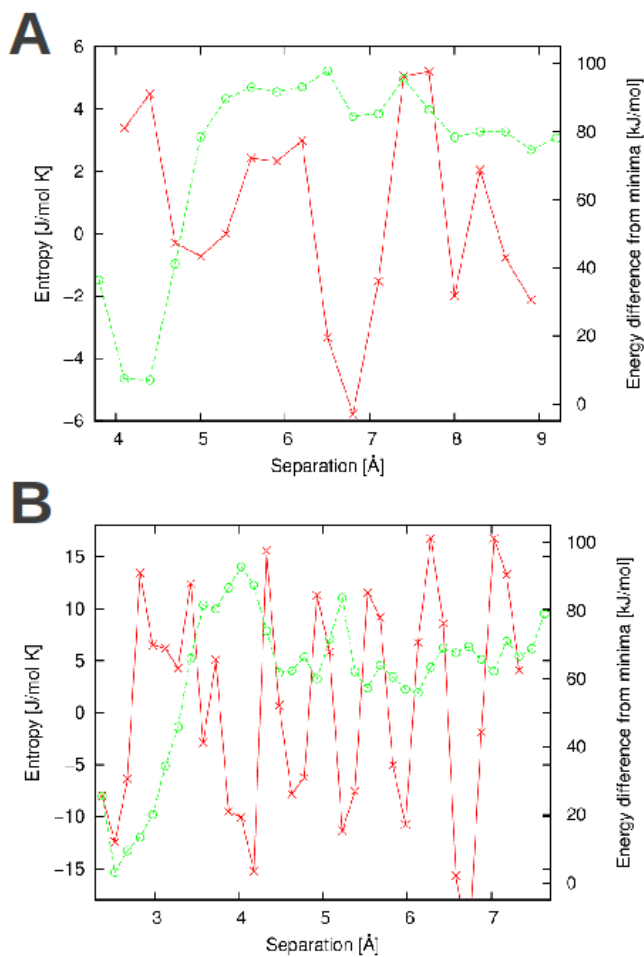


Figure 5.: Variation of entropy (red crosses) and configurational energy (green circles) during TI for (A) mannose and (B) methanoic acid.

The entropy variation for the acid molecule shows far more variation (see Figure 5B) and no clear pattern can be observed. The reason for the spread is not clear as the final configuration energies have the same accuracy as the mannose data but may relate to the more variable configuration energy observed for the adsorption of the acid molecule. Despite this variation the total entropy of the process can be calculated and used for analysis.

3.5 Entropy of Surface Water By performing the same TI for the mannose and acid molecules in vacuum it is possible to estimate the entropic contribution due to the water component of the system. The TI integration gives free energy of binding values of -8.44 kJmol^{-1} and -2.59 kJmol^{-1} respectively for the mannose and methanoic acid molecules in vacuum. Separating out the entropic and enthalpic components generates entropy of binding values, $S_{molecule}$, of $-2.85 \text{ JK}^{-1}\text{mol}^{-1}$ and $-3.50 \text{ JK}^{-1}\text{mol}^{-1}$ for

the mannose and methanoic acid molecules. Assuming,

$$S_{total} = S_{molecule} + nS_{water}, \quad (3)$$

where S_{total} is the total entropy change for binding in the solvated system, S_{water} the entropy change for each water molecule displaced and n is the total number of water molecules displaced, we can estimate the entropy change from the water molecules alone. This produces values of $18.47 \text{ JK}^{-1}\text{mol}^{-1}$ and $13.95 \text{ JK}^{-1}\text{mol}^{-1}$ for the mannose and methanoic acid simulations respectively. These values are positive as would be expected as tightly bound water molecules are being displaced from the surface.

Given the long residence times and highly organised structure of the surface water within the first two layers on the surface it is reasonable to assume that the majority of the entropy change in the water system comes from displacements in these two layers. A total of 3.29 and 2.25 water molecules are displaced from the surface layers by the mannose molecule and acid molecule respectively. Using Equation 3 we can calculate S_{water} per water molecule by dividing the total value by n , the number of water molecules displaced. This gives values of $+5.62 \text{ JK}^{-1}\text{mol}^{-1}$ and $+6.20 \text{ JK}^{-1}\text{mol}^{-1}$ for the mannose and methanoic acid systems respectively.

Previous calculations¹⁴ have assigned a total entropy of $60.0 \text{ JK}^{-1}\text{mol}^{-1}$ to a liquid molecule of water which is divided as $45.4 \text{ JK}^{-1}\text{mol}^{-1}$ (vibrational), $16.1 \text{ JK}^{-1}\text{mol}^{-1}$ (librational) and $8.5 \text{ JK}^{-1}\text{mol}^{-1}$ (rotational). As the binding of the water to the calcite surface is a physisorption process changes to the internal vibrational modes would be small and therefore the entropic changes to the molecule would be expected to be predominately rotational and librational. The librational component, q_l of a particle of mass, m , is defined as:

$$q_l = \left(\frac{2\pi mkT}{h^2}\right)^{3/2}V, \quad (4)$$

which can further divided into a translational, q_t , and configurational, q_c , components defined as:

$$q_t = \left(\frac{2\pi mkT}{h^2}\right)^{3/2}, \quad (5)$$

and,

$$q_c = V, \quad (6)$$

where V is the volume of the system. For a free molecule of water in the bulk V is the specific molecular volume at the given temperature and pressure as listed in Table 1. The change in the entropic components can be examined by studying the rotation and translation of the water and comparing between surface and bulk molecules. The average total rotation of the water molecule (averaging all

three rotational vectors) per timestep is listed in Table 1 for water molecules on the surface or in the bulk during 18 ps of simulation time. As can be seen, the rotation rate of the water molecules is slightly increased by the presence of the surface although both the bulk and surface values are well within their collective error range and therefore we would assume their rotational entropy to be approximately the same. The average displacement of the centre of mass of a water molecule per timestep is listed in Table 1 for water molecules on the surface and in the bulk. This value equates to q_t as it provides a value for the mobility of a molecule. The water molecule has the same velocity on the surface as in the bulk indicating that q_t should be similar for both. No long range diffusion, however, of water molecules is seen on the surface of calcite during the simulations. This indicates an *effective* specific molecular volume for the water molecules on the calcite surface which can be estimated from the mean square displacement (msd) values of the atoms of the water molecules of 14 \AA^3 (Table 1) which is approximately half that of the free bulk water. These results imply that the entropy loss for water molecules on the calcite surface is largely caused by their configurational restrictions which is caused by the structuring of the water. This same structuring is responsible for a large enthalpy gain due to the organisation of the H-bonds between the water molecules and their positioning in relation to the surface ions. Given that the estimated total librational contribution for a bulk water molecule has been calculated as $16.1 \text{ Jmol}^{-1}\text{K}^{-1}$ then the assumption would be that the entropy change for a water molecule adsorbing onto the surface would be less than this value. This compares very well to the value we have calculated from our own method and suggests that this is capturing the main features associated with the adsorption process.

TABLE 1: Data for comparison of Entropic contributions for the water molecules in bulk and within the first two surface layers.

Position	Rotation [degrees/fs] ¹	Displacement [\AA /fs]	Molar Volume [\AA^3]
bulk	2.45 ± 0.37	0.0032 ± 0.002	30.19
surface	2.68 ± 0.80	0.0032 ± 0.002	14.00

3.6 Implications for Molecular Binding When calculating the adsorption energy of molecules at mineral surfaces it is standard to calculate the configurational energy/enthalpy and compare these values - which neglects any entropic contribution to the binding. Our results indicate that molecular adsorption on a solvated calcite surface will generally be a positive entropy process due to the release of the tightly bound water molecules from the surface. Therefore where the adsorption energy is negative for the adsorption of a molecule the free energy of adsorption would also be expected to be negative and

the effect of entropy does not affect the general result of whether binding is favourable or not in systems like calcite where the enthalpy term is large and favourable. Where entropy may become important is in comparison between configurations. It has been highlighted that the adsorption energies are highly dependent on the displacement of water from the calcite surface⁸ and that minimising the disruption and displacement of water molecules from the surface leads to a more negative adsorption energy. This was particularly noticeable for the different binding configurations of OC-17 to the (10.4) calcite surface.¹⁰ The most negative adsorption energy (configuration 1: -422 kJmol⁻¹) was observed for the configuration with only three arginines in contact with the surface and the majority of the protein withdrawn from the surface. In comparison the configuration with the largest number of residues in contact with the surface had the least negative adsorption energy (configuration 3: -53 kJmol⁻¹) despite being in the same planar position (i.e. x and y) on the calcite surface. This was due to the large number of extra water molecules displaced from the calcite surface for the lower adsorption energy configuration compared to the higher adsorption energy configuration. Because these two configurations are displacing a different number of water molecules their entropic components will be different. This then begs the question of whether the entropy will alter which of these configurations has the lowest free energy of adsorption?

It is beyond the realms of practical simulation to attempt a TI on the binding of a large system such as a whole protein to a calcite surface and therefore it is essential to estimate the entropic component. It is reasonable to assume that the entropic contribution for the protein is the same for all the configurations given that the OC-17 protein is extremely rigid and previous analysis found no significant structural changes between the protein bound or unbound in any of the different configurations. As we sample the NVT ensemble, the *pseudo*-free energy of the adsorption can be defined as the Helmholtz Energy, A ,

$$A = U - TnS, \quad (7)$$

where U is the internal energy of the configuration, n is the number of water molecules displaced from the surface and S is the entropy of a single water molecule displaced from the surface. It should be noted that this assumes that each water molecule displaced from the surface undergoes the same entropy change. As the water structure is disrupted by an adsorbing molecule it is reasonable to think that remaining molecules may become either more tightly or more weakly bound to the surface and therefore possess a different entropy but this is beyond the current study. These values are all shown in Table 2 for the two different OC-17 configurations and have been substituted into equation 7 to calculate the *pseudo*-free energy of the adsorption. The values in Table 2 demonstrate that the entropic effects of water displacement do not affect the general conclusions from the configuration adsorption energy. The

difference in free energy of adsorption between the two configurations is 383 kJmol^{-1} compared to 369 kJmol^{-1} for the configuration energy alone. Therefore the effect of the water entropy is relatively minor and has no major effect on the conclusions made previously that configuration 1 binds far more strongly. The size of the water entropy is relatively modest and therefore this should only become a particularly significant factor when the enthalpy of two configurations are close and the difference in the number of water displaced is large. In other cases extrapolating the enthalpy or configuration energy remains viable.

TABLE 2: Values used for the calculation of the free energy of adsorption for ovocleidin-17.

	Number of water molecules displaced n	Total Entropic Contribution (TnS) [kJmol^{-1}]	Internal Energy U [kJmol^{-1}]	Free Energy of Adsorption A [kJmol^{-1}]
configuration 1	21.3	+39.9	-148.8	-188.6
configuration 3	33.9	+63.4	+257.9	+194.5

4. Conclusions

In this paper we have demonstrated how the entropy extraction method of Smith and Haymet can be extended to predict the entropy of molecular binding on calcite surfaces. Our simulations demonstrate, as expected, that the molecules lose entropy on binding to the surface but this is outweighed by a gain in entropy due to the displacement of the surface water away from the calcite. We have estimated that the surface water has lost $\sim 6 \text{ Jmol}^{-1}\text{K}^{-1}$ which is due to a loss of the configurational entropy of the water as it is bound tightly to a given position on the surface. The water molecule does not appear to lose rotational or translational entropy upon binding. By using our estimate of entropy we have been able to calculate an estimate for the free energy of binding for a whole protein on the surface of calcite. Our calculations demonstrate that the entropy gain associated with the displacement of water has no significant effect on the energy differences between the strong and weak binding configurations identified from the configuration energy alone. Where water entropy may become significant is when the two configurations have relatively close energies but significantly different numbers of water are displaced from the surface.

5. Acknowledgements

The authors would like to thank P. Mark Rodger for his initial guidance in this project. This work was supported by the Engineering and Physical Sciences Research Council [grant number EP/I001514/1].

This Programme Grant funds the Materials Interface with Biology (MIB) consortium. Some computer resources on the HPCx service were provided via our membership of the UK's HPC Materials Chemistry Consortium and funded by EPSRC (portfolio grant EP/D504872).

References

- [1] Goobes, R.; Goobes, G.; Campbell, C.T.; and Stayton, P.S. Thermodynamics of statherin adsorption onto hydroxyapatite, *Biochemistry*, **2006**, *45*(17), 5576–5586.
- [2] Campbell, C.T.; and Lytken, O. Experimental measurements of the energetics of surface reactions *Surface Science*, **2009**, *603*(10-12, Sp. Iss. SI), 1365–1372.
- [3] Kerisit, S.; and Parker, S.C. Free Energy of Adsorption of Water and Metal Ions on the 1014 Calcite Surface *Journal of the American Chemical Society*, **2004**, *126*(32), 10152–10161.
- [4] Battle, K.; Salter, E.A.; Edmunds, R.W.; and Wierzbicki, A. Potential of mean force calculation of the free energy of adsorption of Type I winter flounder antifreeze protein on ice *Journal of Crystal Growth*, **2010**, *312*(8), 1257–1261, 17th Amer Conference on Crystal Growth and Epitaxy/14th United States Biennial Workshop on Organometallic Vapor Phase Epitaxy/6th Inter Workshop on Modeling in Crystal Growth, Lake Geneva, WI, AUG 09-14, 2009.
- [5] Piana, S.; Jones, F.; Taylor, Z.; Raiteri, P.; and Gale, J.D. Exploring the role of ions and amino acids in directing the growth of minerals from solution *Mineralogical Magazine*, **2008**, *72*(1), 273–276, 8th International Symposium on the Geochemistry of the Earths Surface (GES-8), London, England, AUG 18-22, 2008.
- [6] Marrink, S.J.; and Berendsen, H.J.C. Simulation of Water Transport Through a Lipid-Membrane *Journal of Physical Chemistry*, **1994**, *98*(15), 4155–4168.
- [7] Laio, A.; and Parrinello, M. Escaping free-energy minima *Proceedings of the National Academy of Sciences of the United States of America*, **2002**, *99*(20), 12562–12566.
- [8] Freeman, C.L.; Asteriadis, I.; Yang, M.; and Harding, J.H. Interactions of Organic Molecules with Calcite and Magnesite Surfaces *Journal of Physical Chemistry C*, **2009**, *113*(9), 3666–3673.
- [9] Elhadj, S.; Salter, E.A.; Wierzbicki, A.; De Yoreo, J.J.; Han, N.; and Dove, P.M. Peptide Controls on Calcite Mineralization: Polyaspartate Chain Length Affects Growth Kinetics and Acts as a Stereochemical Switch on Morphology *Crystal Growth and Design*, **2006**, *6*(1), 6197–201.
- [10] Freeman, C.L.; Harding, J.H.; Quigley, D.; and Rodger, P.M. Simulations of Ovocleidin-17 Binding to Calcite Surfaces and Its Implications for Eggshell Formation *Journal of Physical Chemistry C*, **2011**, *115*(16), 8175–8183.
- [11] Freeman, C.L.; Harding, J.H.; Quigley, D.; and Rodger, P.M. Protein binding on stepped calcite surfaces: simulations of ovocleidin-17 on calcite {31.16} and {31.8} *Physical Chemistry Chemical Physics*, **2012**, *14*(20), 7287–7295.

- [12] Schlitter, J. Estimation of Absolute and Relative Entropies of Macromolecules Using the Variance-Matrix *Chemical Physics Letters*, **1993**, *215*(6), 617–621.
- [13] Harris S.A.; and Laughton, C.A. A Simple Physical Description of DNA Dynamics: Quasi-Harmonic Analysis as a Route to the Configurational Entropy *Journal of Physics-Condensed Matter*, **2007**, *19*(7).
- [14] Irudayam, S.J.; and Henchman, R.H. Entropic Cost of Protein-Ligand Binding and Its Dependence on the Entropy in Solution *Journal of Physical Chemistry B*, **2009**, *113*(17), 5871–5884.
- [15] Irudayam, S.J.; Plumb, R.D.; and Henchman, R.H. Entropic trends in aqueous solutions of the common functional groups *Faraday Discussions*, **2010**, *145*, 467–485.
- [16] Lin, S.T.; Blanco, M.; and Goddard III, W.A. The two-phase model for calculating thermodynamic properties of liquids from molecular dynamics: Validation for the phase diagram of Lennard-Jones fluids *Journal of Chemical Physics*, **2003**, *119*(22), 11792–11805.
- [17] Lin, S.T.; Maiti, P.K.; and Goddard III, W.A. Two-Phase Thermodynamic Model for Efficient and Accurate Absolute Entropy of Water from Molecular Dynamics Simulations *Journal of Physical Chemistry B*, **2010**, *114*(24), 8191–8198.
- [18] Debnath, A.; Mukherjee, B.; Ayappa, K.G.; Maiti, P.K.; and Lin, S.T. Entropy and dynamics of water in hydration layers of a bilayer *The Journal of Chemical Physics*, **2010**, *133*, 174704.
- [19] White, R.P.; and Meirovitch, H. A simulation method for calculating the absolute entropy and free energy of fluids: Application to liquid argon and water *Proceedings of the National Academy of Sciences of the United States of America*, **2004**, *101*(25), 9235–9240.
- [20] Smith, D.E.; Zhang, L.; and Haymet, A.D.J. Entropy of Association of Methane in Water - a New Molecular-Dynamics Computer-Simulation *Journal of the American Chemical Society*, **1992**, *114*(14), 5875–5876.
- [21] Smith, D.E.; and Haymet, A.D.J. Free-Energy, Entropy, and Internal Energy of Hydrophobic Interactions - Computer Simulations *Journal of Chemical Physics*, **1993**, *98*(8), 6445–6454.
- [22] Chialvo, A.A. Determination of Excess Gibbs Free-Energy from Computer-Simulation by the Single Chargeing-Integral Approach .1. Theory *Journal of Chemical Physics*, **1990**, *92*(1), 673–679.
- [23] Mezei, M.; and Beveridge, D.L. Free Energy Simulations *Annals of the New York Academy of Sciences*, **1986**, *482*, 1–23.
- [24] Cornell, W.D.; Cieplak, P.; Bayly, C.I.; Gould, I.R.; Merz Jr., K.M.; Ferguson, D.M.; Spellmeyer, D.C.; Fox, T.; Caldwell, J.W.; and Kollman, P.A. A 2nd Generation Force-Field for the Simulation of Proteins, Nucleic-Acids, and Organic-Molecules *Journal of the American Chemical Society*, **1995**, *117*, 5179–5197.

- [25] Pavese, A.; Catti, M.; Price, G.D.; and Jackson, R.A. Interatomic Potentials for CaCO₃ Polymorphs (Calcite and Aragonite) Fitted to Elastic and Vibrational Data *Physics and Chemistry of Minerals*, **1992**, *19*, 80–87.
- [26] Pavese, A.; Catti, M.; Parker, S.C.; and Wall, A. Modelling of the thermal dependence of structural and elastic properties of calcite, CaCO₃ *Physics and Chemistry of Minerals*, **1996**, *23*, 89–93.
- [27] Jorgensen, W.L.; Chandrasekhar, J.; Madura, J.D.; Impey, R.W.; and Klein, M.L. Comparison of simple potential functions for simulation liquid water *Journal of Chemical Physics*, **1983**, *79*, 926–935.
- [28] Freeman, C.L.; Harding, J.H.; Cooke, D.C.; Elliot, J.A.; Lardge, J.S.; and Duffy, D.M. New Forcefields for Biomineralisation Processes *Journal of Physical Chemistry C*, **2007**, *111*, 11943–11951.
- [29] Watson, G.W., Kelsey, E.T.; deLeeuw, N.H.; Harris, D.J.; and Parker, S.C. Atomistic Simulation of Dislocations, Surfaces and Interfaces in MgO

Journal of the Chemical Society: Faraday Transactions, **1996**, *92*, 433.
- [30] Smith, W.; and Forester, T.R. DL_POLY_2.0: A general-purpose parallel molecular dynamics simulation package *Journal of Molecular Graphics*, **1996**, *198/199*, 796–781.
- [31] Yang, M.; Harding, J.H.; and Stipp, S.L.S. Simulations of monosaccharide on calcite surfaces *Mineralogical Magazine*, **2008**, *72*(1), 295–299, 8th International Symposium on the Geochemistry of the Earths Surface (GES-8), London, England, AUG 18-22, 2008.